

MAY 31 1946

NATIONAL ADVISORY COMMITTEE
FOR AERONAUTICS

TECHNICAL NOTE

No. 1066

STRESSES AROUND LARGE CUT-OUTS
IN TORSION BOXES

By Paul Kuhn and Edwin M. Moggio

Langley Memorial Aeronautical Laboratory
Langley Field, Va.



Washington
May 1946

NA CA LIBRARY
LANGLEY MEMORIAL AERONAUTICAL
LABORATORY
Langley Field

NATIONAL ADVISORY COMMITTEE FOR AERONAUTICS

TECHNICAL NOTE NO. 1066

STRESSES AROUND LARGE CUT-OUTS

IN TORSION BOXES

By Paul Kuhn and Edwin M. Moggio

SUMMARY

The problem treated in this paper is that of the stresses in a torsion box with a large rectangular cut-out. The theoretical treatment is confined to stresses termed the "primary stresses." Comparison of the theoretical results with strain-gage data for a series of cut-outs indicates that the primary stresses are probably adequate for designing the major part of the structure, the only important exception being in the design of the cover sheet in the full section adjacent to the cut-out.

INTRODUCTION

The importance of cut-out problems in aircraft shell analysis is well known. Many of these problems can be treated with sufficient accuracy as stress problems in a plane and are then amenable to relatively simple treatment. A cut-out in a torsion box, however, can be dealt with in this manner only if the cut-out is small. A solution that remains valid for large cut-outs requires considerations of the action of the entire space structure, and a complete analytical solution would be very cumbersome. A practical expedient for alleviating this difficulty is to effect the solution in steps comparable to those taken in the analysis of stiff-jointed trusses. In truss analysis, the first step consists in finding the so-called "primary stresses" by simple methods. In the second and more difficult step, the so-called "secondary stresses" are found. These stresses are theoretically quite large, sometimes larger than the primary stresses, but designs having satisfactory static strengths can often be produced with very little labor expended on the determination of the secondary stresses by using approximate methods and by taking advantage of the fact that yielding tends to eliminate stress.

concentrations. Even when this fortunate situation does not exist, the separate calculation of the primary stresses offers such important advantages in clarifying the calculations that it is standard procedure for trusses.

For similar reasons, the present paper gives what might be called a primary-stress analysis for the torsion box with a cut-out of any size. A study of the strain-gage data presented indicates that the stresses obtained from the primary-stress analysis are probably adequate for designing the major part of the structure affected by the cut-out, the only important exception being the cover sheet in the full box section adjacent to the cut-out.

SYMBOLS

Symbols, including subscripts, relating to the geometry of the structure are shown in figures 1 and 2. Conventions for coordinates are shown in figure 3.

- a length of closed box, inches
- b width of box (shear web to shear web), inches
- c depth of box (cover sheet to cover sheet), inches
- d half-length of cut-out, inches
- h width of net section (one side), inches
- k fraction of total torque carried by shear webs in cut-out bay
- q shear flow (running shear), pounds per inch
- T_0 "basic" shear flow, pounds per inch ($T/2bc$)
- t thickness of wall, inches
- \bar{y} distance from neutral axis of net section to coaming stringer, inches
- A cross-sectional area of member carrying direct stress, square inches

A _o	enclosed area of torsion box (bc), square inches
C, C'	coefficients defined in text
E	Young's modulus, kips per square inch
G	shear modulus, kips per square inch
I	moment of inertia of beam, inches ⁴
M	bending moment in beam, inch-kips
N.A.	neutral axis
Q	static moment about neutral axis of the portion of beam cross-section lying between extreme fiber and fiber under consideration, inches ³
S	surface area of one wall in one bay, square inches
T	torque, inch-kips
V	transverse shear force in beam, kips
W	internal work stored, kip-inches
σ	direct stress, ksi
τ	shear stress, ksi.

The quantities M, I, Q, and V apply to the net section of the cover considered as a beam bending in its own plane.

Station numbers indicate the distance in inches from the transverse center line of the box.

METHOD OF THEORETICAL ANALYSIS

The problem considered is that of a torsion box of rectangular cross-section with a centrally located rectangular cut-out in one cover (fig. 1). Torque-transfer bulkheads at the ends of the cut-out separate the box into two closed bays and one open or cut-out bay. The structure is at first assumed to be symmetrical about a

transverse plane as well as about a longitudinal plane. Procedures for taking into account some dissymmetries will be indicated.

Theory of Symmetrical Structure

In order to facilitate the calculation of the primary stresses in the structure, all direct stresses are assumed to be carried by concentrated main flange members as indicated in figure 2. The contributions of such stringers as may be present and of the sheet to the direct stresses are taken into account by making suitable additions to the areas of the actual main flanges. This method of simplifying the box structure has been used extensively by many authors for similar problems and is analogous to the procedure of adding one-sixth of the web area to each flange area for the analysis of a plate-girder.

It may be noted in figure 2 that the "coaming" stringers (stringers bounding the cut-out) of the simplified structure do not extend beyond the cut-out, although good design practice would require them to extend beyond the cut-out in an actual structure. This simplification was based on the observation that in actual structures the stresses in these extensions decrease rapidly with increasing distance from the cut-out and consequently furnish only a small contribution to the strain energy of the torsion box. It is necessary, of course, to assume that the cap strips of the torque-transfer bulkheads have sufficient stiffness against bending in the plane of the cover to function as abutments for the coaming stringers; infinite stiffness will be assumed in the following theoretical development.

In a rectangular torsion box of constant section without a cut-out, the division of the applied torque T between the two pairs of walls is statically determinate; the pair of cover sheets carries one-half of the torque, the pair of shear webs the other half. In a torsion box with a cut-out, the division of the torque is statically indeterminate. If kT denotes that part of the torque that is carried by the shear webs in the cut-out bay, the part carried by the uncut cover and the net section of the cut cover in the same bay is then $(1-k)T$. Figure 3(a) shows the shear flows in the cut-out bay expressed in terms of k and the "basic" shear flow

$$q_0 = \frac{T}{2bc} \quad (1)$$

that would exist if there were no cut-out. With the shear flows thus defined, the forces or stresses in the coaming members and in the corner flanges can be found by applying the equilibrium equation $\sum X = 0$ to these members. Finally, the shear flows in the closed box can be established from the condition that the internal torque must equal the applied torque and from the equilibrium condition $\sum X = 0$ applied to the corner flange. All the shear flows and direct stresses are thus found in terms of the applied torque and the fraction k as shown in figure 3.

The fraction k is statically indeterminate and is calculated by applying the Principle of Least Work

$$\frac{\partial W}{\partial k} = 0 \quad (2)$$

The internal work W is

$$W = \int \frac{\tau^2}{2G} dV + \int \frac{\sigma^2}{2E} dV \quad (3)$$

where dV is the elemental volume of material stressed and the integration extends over the entire structure. The expression (2) can therefore be written in the form

$$\frac{\partial W}{\partial k} = \int \frac{\tau}{G} \frac{\partial \tau}{\partial k} dV + \int \frac{\sigma}{E} \frac{\partial \sigma}{\partial k} dV = 0 \quad (4)$$

which may be transformed into

$$\frac{\partial W}{\partial k} = \sum \frac{q}{G} \frac{\partial q}{\partial k} \frac{S}{t} + \int \frac{\sigma}{E} \frac{\partial \sigma}{\partial k} A dx = 0 \quad (5)$$

where S is the surface area of a given wall in a given bay, no integrations being required for the shear stresses,

which are constant in each wall of a given bay. By inserting in expression (5) values for q and σ from figures 3(a) and 3(b) and separating terms, it is readily found that

$$k = \frac{\sum_{l=1}^{10} c'}{\sum_{l=1}^{10} c} \quad (6)$$

where

$$c_1 = \frac{4c}{t_{cl}} \quad c'_{11} = 0$$

$$c_2 = \frac{2b}{t_{bl}} \quad c'_{12} = c_2$$

$$c_3 = \frac{b^2}{ht_h} \quad c'_{13} = c_3$$

$$c_4 = \frac{4bd}{at_{b2}} \quad c'_{14} = \frac{1}{2} \left(1 + \frac{a}{d}\right) c_4$$

$$c_5 = \frac{4cd}{at_{c2}} \quad c'_{15} = \frac{1}{2} \left(1 + \frac{a}{d}\right) c_5$$

$$c_6 = \frac{2bc}{dt_B} \left(1 + \frac{d}{a}\right)^2 \quad c'_{16} = \frac{1}{2} c_6$$

$$c_7 = \frac{G}{3E} \frac{b^2 d^2}{A_1 h^2} \quad c'_{17} = c_7$$

$$c_8 = \frac{G}{3E} \frac{d^2}{A_2} \left(2 + \frac{b}{h}\right)^2 \quad c'_{18} = c_8 \frac{b}{b + 2h}$$

$$C_9 = \frac{16G}{3E} \frac{d^2}{A_3}$$

$$C'9 = C_9$$

$$C_{10} = \frac{32G}{3E} \frac{ad}{A_4}$$

$$C'10 = \frac{1}{2} C_{10}$$

When the net section is very narrow, a more convenient procedure is to add C_7 to C_8 as well as $C'7$ to $C'8$ and to split the resulting terms into two new terms that can be written as

$$C_{7a} = \frac{Gb^2d^2}{3EI}$$

$$C'7a = C_7a$$

$$C_{8a} = \frac{4Gd^2}{3EA_2} \frac{(b + h)}{h}$$

$$C'8a = \frac{2G}{3E} \frac{bd^2}{A_2h}$$

where I is the moment of inertia of the net section (one side) which is considered a beam that resists bending in the plane of the cover sheet. Under these conditions, h should be considered the "effective" width of net section resisting the transverse shear force and ht_h the effective shear area of the net section. In all cases, the spar cap must be considered a part of the net section and, consequently, h cannot become zero, although it may become very small compared with b . To define h and th with any degree of accuracy when the net section is narrow may be difficult, but this difficulty is immaterial because the terms C_3 and C_{8a} containing h and th are then small compared with C_{7a} unless the length of the cut-out becomes very small at the same time.

In an actual structure, the walls carry not only shear stresses but also direct stresses and, in most cases, stringers carrying direct stresses are attached to the cover sheets. In order to account for these stresses, the flange area in the simplified structure is taken as the sum of the flange area in the actual structure and the "effective area" of the cover sheet and stringers. In plate-girder design, the effective area of the web is taken as 1/6 of the actual area. Experiments have shown that a smaller fraction should be used for the box covers

(reference 1); a value of 1/20 is suggested if the length-width ratio of the full section of the cover is more than 2, and this value should be reduced for smaller length-width ratios.

Deviations from Symmetry

Deviations from symmetry in the actual structure may be approximately accounted for in the usual manner by using average values. Since all the coefficients are added, an inaccuracy in one coefficient caused by averaging will normally have no serious consequences on the final result. The proper procedure for taking account of dissymmetries in sheet thicknesses t and areas A would be to divide the appropriate coefficient C into two parts; for instance, if the top and bottom cover sheet in the closed box are not equal, the coefficient

$$C_4 = \frac{4bd}{at_{b2}}$$

would be replaced by

$$C_4 = \frac{2bd}{at_{b2\text{top}}} + \frac{2bd}{at_{b2\text{bottom}}}$$

If the structure is not symmetrical about the transverse plane through the middle of the cut-out, the direct stresses will not be zero at this plane; that is, the point of inflection of the beams is not at the middle of the cut-out. In such a case, an arbitrary transverse plane is assumed to separate the structure into two parts, and a value of k is computed for each part. The plane of separation is then shifted until the values of k for the two parts of the structure become equal.

TEST SPECIMEN AND PROCEDURE

The test specimen was the rectangular torsion box shown in figure 4, loaded by couples at the two ends so that there was no restraint against warping of the cross section.

The box was tested in five conditions, the main differences being in the width of the cut-out and in the bulkheads. The widths of the cut-outs are defined by the widths h of the net section, which are given together with all other basic data needed for analysis in table I. The end bulkheads were attached directly to the skin in all cases. The intermediate bulkheads were "floating" on the Z-stringers as shown in the lower right corner of figure 4. The torque-transfer bulkheads were of construction similar to that of the intermediate bulkheads but were floating only on the bottom stringers; at the top, they were attached directly to the skin by means of the transverse coaming members. For case 5, the aluminum-alloy torque-transfer bulkheads were removed and replaced by steel bulkheads attached to the bottom and top skins as shown in the upper left corner of figure 4. The two intermediate bulkheads in the region of the cut-out were removed after the test of case 3. For convenience of reference, the condition of the bulkheads is indicated by the diagrams at the top of figures 5 to 9. No special reinforcements were provided along the longitudinal edges of the cut-out (the Z-stringers serving as coaming stringers) in order to have high direct stresses in the net section and thus to obtain a sensitive check on the theory.

The load was measured by a dynamometer to an accuracy somewhat better than 1 percent. Strains were measured with Tuckerman optical strain gages of 2-inch gage length with a minimum reading of 20 psi. Longitudinal direct strains were measured by gages located over the Z-stringers. The shear strains were obtained from strain gages located on the sheet between stiffeners and oriented at 45° and 135° to the axis of the box. A load-strain plot was made for each gage, and the slope of the straight line through the test points was used to determine the strain at the maximum torque used. Readings were rejected if the straight line missed the origin by more than 100 psi, or if the points did not fall on a straight line within a scatter limit of less than about 60 psi.

Strain readings were taken around the entire perimeter and along the entire length of the box. Because the box was doubly symmetrical, the readings obtained in the four quadrants could be reduced by averaging to a single quadrant with an appreciable increase in reliability of the final result. For converting strains to stresses, Young's modulus was taken as 10,600 ksi and the shear modulus as 4,000 ksi.

ANALYSIS OF RESULTS

Theoretical Calculations

The basic data used in applying the proposed method of analysis are given in table I. The width h of the net section was taken as the distance between the centroid of the Z-stringer acting as coaming member and the centroid of the steel angle forming the corner flange. The effective area of this steel angle was taken as three times the actual area. The presence of all full-floating bulkheads was disregarded in the calculations because inspection of the test data indicated no discontinuity in the stresses at station 42.75, where these bulkheads were located. (See, for instance, fig. 5.) The equivalent thickness t_B of the semifloating torque-transfer bulkheads was estimated as follows.

The Z-stiffeners deform while transmitting a shear force from the bulkhead to the skin as indicated in figure 10. By special tests on a Z-stiffened panel it was established that this deformation can be calculated on the assumption that the web of the Z-stiffener is built-in at both ends and that the effective width of the web partaking of the deformation is equal to 0.7 the depth of this web if the stiffeners stop at the bulkhead and 1.4 times this depth if the stiffeners continue well beyond the bulkhead. (A similar test with hat-section stiffeners gave a coefficient of 0.9 instead of 0.7, probably because the fixation of the web at the closed end of the hat is more nearly perfect than on the Z-stiffener.) With these data, the displacement of the stiffeners under a unit tangential force acting along the edge of the bulkhead was computed. This displacement was divided by the depth c of the box to obtain an "equivalent shear strain" of the bulkhead, which was used in turn to compute the equivalent thickness.

The calculated values of the coefficients C and the fractions k are shown in table II. Inspection of the table indicates that in case 1, the small equivalent thickness of the bulkhead makes the coefficient C_6 predominant; as a result, the value of k is only slightly above 0.5; that is to say, the division of the torque between the cover walls and the shear webs does not differ greatly from the division that would be found in a closed

box. As the cut-out becomes larger (case 2), the term C_7a containing the bending stiffness of the net section against lateral bending becomes appreciable, and in case 3 this term becomes very large and the value of k thus becomes much larger. The physical interpretation of this result is that the shear webs now carry a larger portion of the torque. Case 4 is identical with case 3 insofar as the theoretical calculation is concerned. In case 5, where the extra flexibility of the bulkheads resulting from their floating arrangement has been eliminated, the lack of lateral bending stiffness in the net section with the corresponding predominance of C_7a causes k to come very close to unity; that is, the shear webs carry nearly the entire torque.

In table III are shown the calculations of the shear flows in the individual walls and of the stresses in the coaming stringers. The calculated shear flows may be compared directly with the average experimental shear flows. On the net section, it was not possible to obtain experimentally the average shear flow over the entire section, because the section is too narrow to accommodate an adequate number of strain-gage stations. In order to overcome this difficulty, values of the static moment Q were calculated for each strain-gage station used, and these values were averaged at any given cross section to obtain the value of Q_{av} given in the table. The shear flow q_h was then obtained by multiplying the transverse shear force V acting on one side of the net section by Q_{av} and dividing by I . The shear flow q_h calculated in this manner may be compared with the experimental shear flow obtained by averaging the results from the strain gages at the cross section being considered.

The stresses in the coaming stringers were calculated for one cross section by the formula

$$\sigma = \frac{Vx\bar{y}}{I}$$

where x is the distance of the cross section chosen from the middle of the cut-out. The cross section chosen is the strain-gage station nearest the end of the cut-out, so that a direct comparison between calculated and experimental stresses may be made as shown in the last column of table III.

Comparison Between Theoretical and Experimental

Average Shear Flows

Figures 5 to 9 show the theoretical and the experimental values of the average shear flows in the walls of the test specimen for the five test cases. In a comparison of theoretical and experimental results, the following observations concerning the experimental values should be borne in mind.

The reliability and therefore the relative weight of the experimental points varies widely because of the large variation in the number of gage stations represented by one point on these figures. One point for the cover sheet of the closed-box region or for the bottom cover sheet represents 15 gage stations at two sections, or a total of 30 gage stations. One point for the shear web represents four quadrants with 3 gage stations each, or a total of 12 gage stations. One point for the net section of the top cover sheet represents four quadrants with 3 stations each in case 1, 2 stations each in case 2, and one station each in cases 3, 4, and 5, or totals of 12, 8, and 4 stations, respectively. For points lying on the center line, the numbers given for each case must be divided by two.

The stresses in the shear webs at station 0 and 12.5 in cases 3, 4, and 5 appear to be too high, and a static check of internal against external torque indicates something amiss at these stations. The stresses are believed to be too high as a result of buckling of the shear webs. Rigid-body strain gages lying across a buckle indicate a fictitious compressive strain, which results in exaggerated values of shear stress. Approximate calculations indicated that buckles about $1/64$ to $1/32$ inch deep over a 2-inch gage length might account for the excess of measured stress over calculated stress. Buckles of this depth might well escape casual visual inspection during the test. The stress indicated ranges roughly from 0.65 to 0.85 of the theoretical critical stress, which is probably sufficiently high to develop buckles in a structural element since laboratory tests made for the specific purpose of checking the theory of critical shear stress showed that buckling occurred at stresses below 0.60 of the theoretical values (reference 2). The possibility also exists that some progressive lowering of the buckling stress might have resulted from the repeated loading in the course of testing.

Finally, it should be remembered that the net sections have extreme proportions considered as beams. (See fig. 11.) The proportions are obviously such that close agreement with the ordinary bending theory can hardly be expected.

If all these considerations concerning the experimental values are kept in mind, the agreement between calculated and experimental shear flows may be considered satisfactory. The most noticeable discrepancies appear in the extreme cases where very flexible (semifloating) bulkheads are used to close off a practically full-width cut-out, a combination not likely to be found in practice. In these cases (particularly cases 3 and 4) there was apparently some tendency for the walls of the box to act as a series of very flexible torque-transfer bulkheads and thus to produce a less abrupt change of stress distribution at the end of the cut-out than is produced by the stiff bulkhead in case 5.

In figures 5 and 6 the shear flows in the closed box do not differ greatly from the basic shear flow q_0 obtained by applying formula (1) to the closed box. This agreement might be considered to justify use of this elementary method of analysis for all very large cut-outs approaching the limiting condition of a full-width cut-out. Examination of table 2 indicates, however, that such a conclusion would be erroneous, because the close agreement with elementary theory in the closed box is a result of the fact that the fraction k is close to 0.5 and this value in turn is a result of the extreme flexibility of the torque-transfer bulkheads. A re-computation of k for these two cases with stiff bulkheads assumed indicates appreciable deviations of the shear flows from the values given by the elementary formula.

Detailed Distribution of Shear Stresses

The details of the shear-stress distribution are shown in figures 12 to 15 in the form of stress plots over the developed perimeter of the box. The stresses for cases 3 and 4 are shown in a single figure for identical applied torques in order to demonstrate that the removal of the two bulkheads in the cut-out region had only minor local effects. Inspection of these figures indicates that in some regions the shear stress is fairly uniformly distributed over the wall, and consequently the average shear stress obtained by the method of analysis

developed in this paper may be adequate for design purposes. In other regions, however, the distribution is quite nonuniform, and the proposed primary-stress theory must be supplemented by another theory giving the distribution of the stresses and their peak values.

The following tentative conclusions were drawn from these data (figs. 12 to 15) concerning the adequacy of the method for design:

(1) For the shear web, the calculated average stress is probably adequate for design.

(2) For the bottom cover, the calculated average stress is probably adequate for design, except that in the cut-out bay allowance might have to be made for stresses of the order of q_0 near the edges of the sheet.

(3) In the net section of the top cover near the middle of the cut-out, the shear stresses calculated by VQ/It are probably adequate for design; near the ends of the cut-outs, the actual distribution of the shear appears to be almost opposite to the calculated distribution, the maximum occurring near the corner of the cut-out in the bay next to the coaming member instead of near the neutral axis. In design, allowance should be made for this deviation from the theory.

(4) In the gross section of the top cover, the chordwise distribution is very nonuniform, and the present theory is inadequate for design. If the cut-out is nearly full-width, the nonuniformity disappears at a rather short distance from the end of the cut-out; if the cut-out is not quite so wide, the nonuniformity persists to a larger distance.

Distribution of Direct Stresses

The distribution of the measured direct stresses is shown in figures 16 to 20. Calculated stresses are shown for the coaming stringers in the region of the cut-out and for the corner flanges. The calculated flange stresses are discontinuous at the ends of the cut-outs because the simplified theory used assumes that the cap strip of the torque-transfer bulkhead transmits the reactions from the net section of the cut-out bay to the corner flanges of

the closed bays. Actually, these reactions are diffused to some extent; the length of the diffusion zone may be estimated roughly to be twice the width h of the net section and within this zone the experimental stresses in the flange could be expected to agree with the calculated stresses only if the measurements were taken along the neutral axis of the net section for lateral bending.

The general agreement between calculated and experimental stresses may be considered fair, particularly in view of the fact that the results of the calculations are quite sensitive in some cases to small changes in the given data. The stress in the coaming stringer is proportional to $(1-k)$ as indicated in figure 3(b); for large cut-outs, the value of k closely approaches unity and, consequently, the accuracy of the computed stringer stresses is of a lower order of magnitude than that of the factor k . In cases 1 and 2 (figs. 16 and 17) it may also be noted that the experimental neutral axis agrees fairly well with the calculated axis. In the remaining cases no such comparison may be made; there are only two experimental points at any section, and the point on the corner flange may not be used to establish the transverse distribution of stress because the stress at this point is affected by bending in the plane of the shear web as well as by bending of the net section in the plane of the cover.

In figure 21 are shown the stresses in the coaming stringers reduced to the same applied torque for easier comparison. When the stresses rise to a high peak, they also decrease very rapidly in the region of the closed box. As mentioned in the section "Method of Theoretical Analysis," this fact furnishes the justification for omitting the extensions of the coaming stringers from the simplified or primary structure used for the analysis. Some of the experimental curves are terminated just to either side of the end of the cut-out; the points of termination are the last experimental points, and extrapolation beyond these points was considered too unreliable because the curves are too steep. Of some interest is the great decrease in stringer stress resulting from replacement of the semifloating torque-transfer bulkhead (case 4) by a stiff bulkhead (case 5).

CONCLUSIONS

From a study of the test results and the comparison between experimental and calculated stresses, the following conclusions were drawn concerning the stresses existing in a three-bay rectangular box with a rectangular cut-out in the middle bay when the box is subjected to pure torque loading in the elastic range:

1. The theory presented appears to be adequate for calculating the transverse shear forces in all the component walls of the structure. When the shear force in the net section of the cut-out cover has been found, the shear stresses and the direct stresses in this section can be computed by standard beam theory.
2. The stresses obtained from the theory are probably adequate for designing all components of the structure excepting the gross section of the cut-out cover, where the distribution of the shear stresses deviates so much from uniformity that an additional theory of secondary stresses must be developed.

Langley Memorial Aeronautical Laboratory
National Advisory Committee for Aeronautics
Langley Field, Va., February 26, 1946

REFERENCES

1. Kuhn, Paul; and Brilmyer, Harold G.: Stresses near the Juncture of a Closed and an Open Torsion Box as Influenced by Bulkhead Flexibility. NACA ARR No. L5G18, 1945.
2. Bollenrath, F.: Wrinkling Phenomena of Thin Flat Plates Subjected to Shear Stresses. NACA TM No. 601, 1931.

TABLE I
BASIC DATA

Item	Case 1	2	3	4	5
a, in.	35.5	35.5	35.5	35.5	34.0
b, in.	51.4	51.4	51.4	51.4	51.4
c, in.	10	10	10	10	10
d, in.	24.5	24.5	24.5	24.5	26.0
h, in.	11.12	6.62	2.12	2.12	2.12
t, in.	.063	.063	.063	.063	.063
t_B , in.	.00194	.00194	.00194	.00194	.375
\bar{y} , in.	8.823	5.581	1.929	1.929	1.929
d/a	.691	.691	.691	.691	.765
q_o , $\frac{lb}{in.}$	97.0	90.3	69.3	62.5	62.5
A_1 , sq in.	.200	.152	.105	.105	.105
A_2, A_3, A_4 , sq in.	1.59	1.59	1.59	1.59	1.59
A_o sq in.	.514	.514	.514	.514	.514
I, in. ⁴	36.75	10.03	1.01	1.01	1.01
Q_{av} , in. ³	3.253	1.443	.302	.302	.302
T, kip-in.	99.75	92.70	71.30	64.12	64.12
τ_o , ksi	1.540	1.432	1.100	0.991	0.991

NATIONAL ADVISORY
COMMITTEE FOR AERONAUTICS

TABLE II
CALCULATION OF k

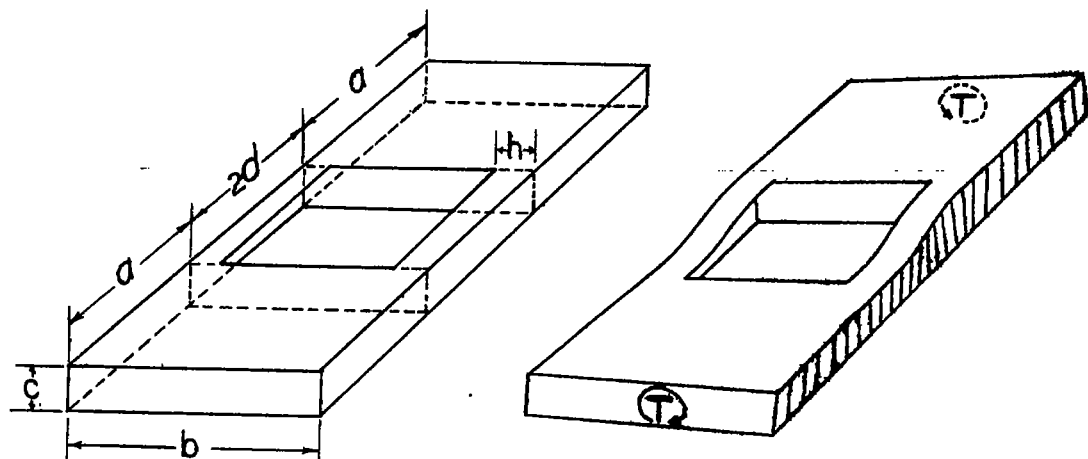
Coefficient	Formula	Case 1	Case 2	Case 3	Case 4	Case 5
c_1	$\frac{4e}{t_{cl}}$	635	635	635	635	635
c_2	$\frac{2b}{t_{bl}}$	1632	1632	1632	1632	1632
c_3	$\frac{b^2}{ht_h}$	3770	6330	19780	19780	19780
c_4	$\frac{4bd}{at_{b2}}$	2250	2250	2250	2250	2500
c_5	$\frac{4cd}{at_{c2}}$	438	438	438	438	486
c_6	$\frac{2be}{dt_B} \left(1 + \frac{d}{a}\right)^2$	61780	61780	61780	61780	328
c_{7a}	$\frac{G}{3E} \frac{b^2 d^2}{I_p}$	5420	19870	197310	197310	222210
c_{8a}	$\frac{4a}{3E} \frac{d^2(b+h)}{A_2 h}$	1070	1663	4789	789	5394
c_9	$\frac{16}{3} \frac{G}{E} \frac{d^2}{A_3}$	759	759	759	759	855
c_{10}	$\frac{32}{3} \frac{G}{E} \frac{da}{A_1}$	2200	2200	2200	2200	2240
$\sum c$		79954	97557	291573	291573	256060
$c'2$	c_2	1632	1632	1632	1632	1632
$c'3$	c_3	3770	6330	19780	19780	19780
$c'4$	$\frac{1}{2} \left(1 - \frac{a}{d}\right) c_4$	-505	-505	-505	-505	-384
$c'5$	$\frac{1}{2} \left(1 + \frac{a}{d}\right) c_5$	536	536	536	536	561
$c'6$	$\frac{1}{2} c_6$	30890	30890	30890	30890	164
$c'7a$	c_{7a}	5420	19870	197310	197310	222210
$c'8a$	$\frac{2}{3} \frac{G}{E} \frac{d^2 b}{A_2 h}$	438	737	2300	2300	2590
$c'9$	$\frac{1}{2} c_9$	380	380	380	380	428
$c'10$	$\frac{1}{2} c_{10}$	1100	1100	1100	1100	1120
$\sum c'$		43661	60970	253423	253423	248101
k	$\frac{\sum c'}{\sum c}$.5461	.6250	.8692	.8692	.9689

TABLE III
CALCULATION OF SHEAR FLOWS AND STRINGER STRESSES

Case	k	$(1 - k)$	$(2k - 1)$	$\frac{d}{a}$	$\frac{d}{a}(2k - 1)$	$1 - \frac{d}{a}(2k - 1)$	$1 + \frac{d}{a}(2k - 1)$	q_o (lb/in.)	q_{c2} (lb/in.)	q_{b2} (lb/in.)	q_{b1} (lb/in.)
1	.5461	.4539	.0922	.691	.0636	.9364	1.064	97.0	90.8	103.2	88.1
2	.6250	.3750	.2500	.691	.1725	.8275	1.173	90.3	74.7	105.9	67.7
3	.8692	.1308	.7384	.691	.5095	.4905	1.510	69.3	34.0	104.6	18.1
4	.8692	.1308	.7384	.691	.5095	.4905	1.510	62.5	30.7	94.3	16.4
5	.9689	.0311	.9378	.765	.7174	.2826	1.717	62.5	17.7	107.3	3.89

Case	q_{c1} (lb/in.)	$T/2e$	V (lb)	Q_{av} in. ³	q_h (lb/in.)	I in. ⁴	\bar{y} (in.)	x (in.)	σ_{calc} (lb/in.)	σ_{exp} (lb/in.)	$\frac{\sigma_{calc}}{\sigma_{exp}}$
1	105.9	4988	2264	3.253	200.4	36.75	8.823	23.5	12770	17000	.751
2	112.9	4635	1738	1.443	250.0	10.03	5.581	22.5	21760	21000	1.038
3	120.5	3565	466.3	.302	139.4	1.01	1.929	23.5	20930	24800	.844
4	108.7	3206	419.4	.302	125.4	1.01	1.929	23.5	18820	20400	.923
5	121.1	3206	99.7	.302	29.8	1.01	1.929	23.5	4475	5500	.814

NATIONAL ADVISORY
COMMITTEE FOR AERONAUTICS



(a) Undeformed state.

(b) Deformed state.

Figure 1.- Torsion box with cut-out.

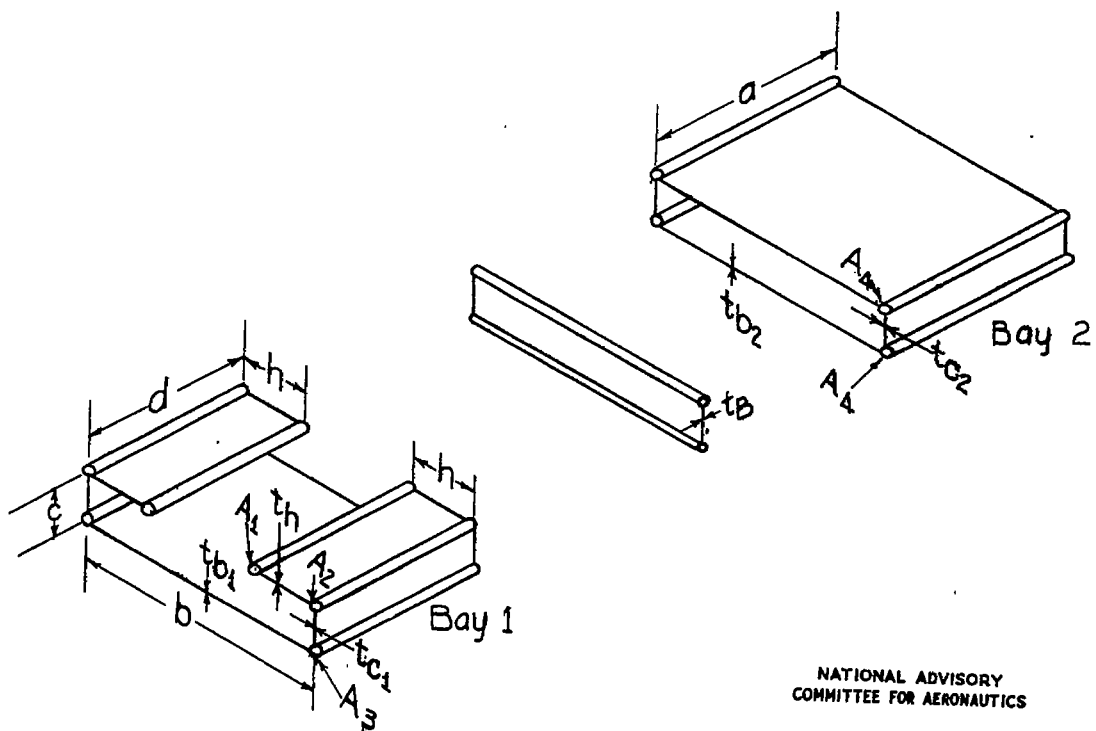
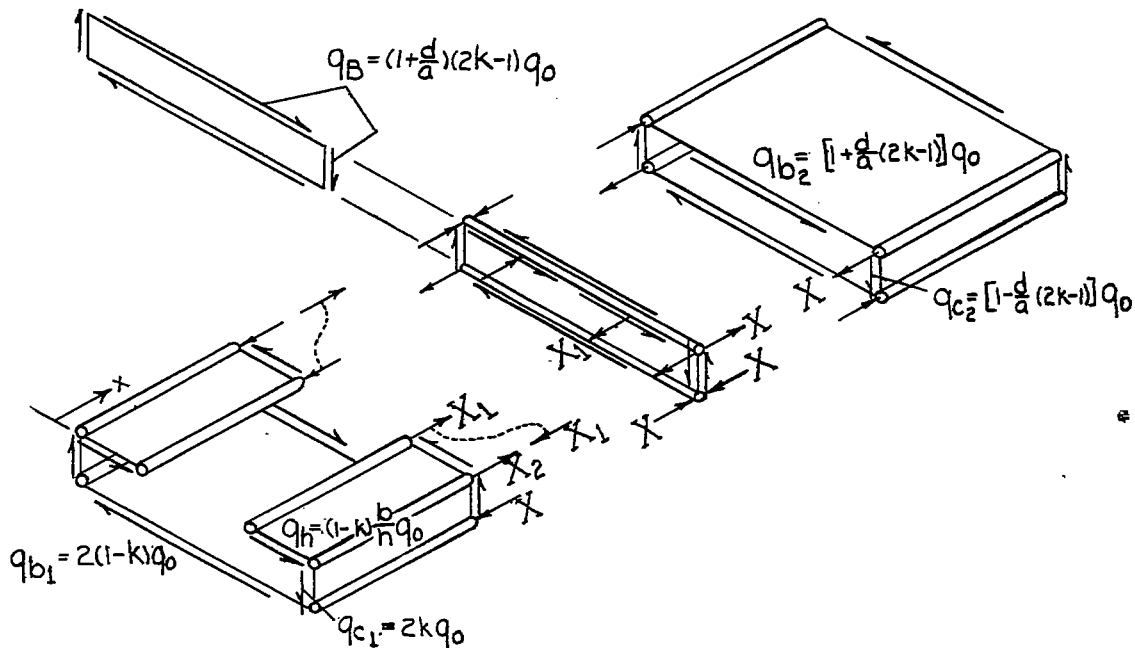
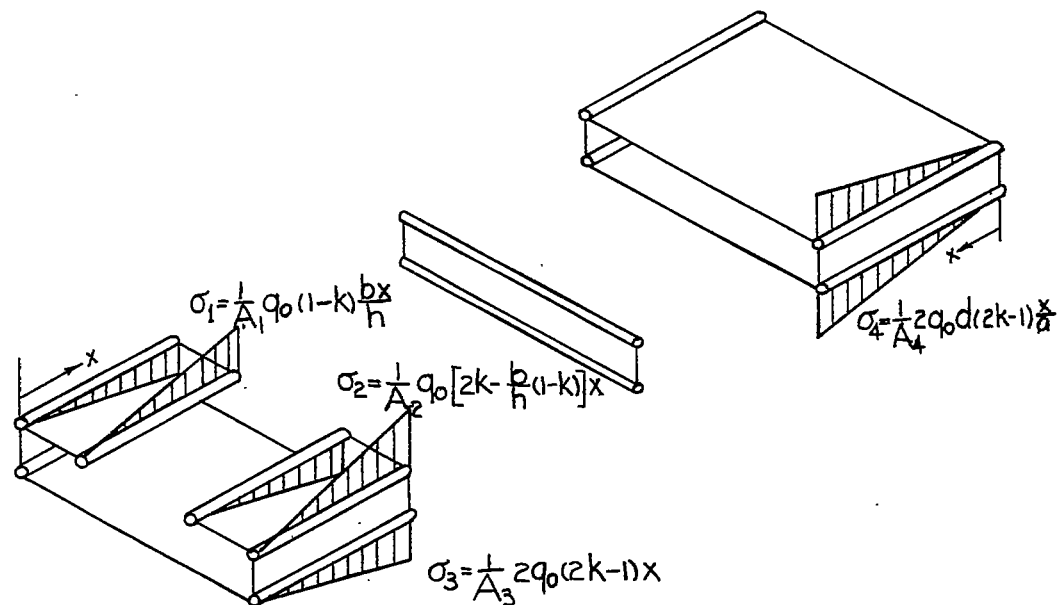


Figure 2.- Exploded view of simplified box structure.



(a) Shear flows and flange forces.



(b) Direct stresses.

NATIONAL ADVISORY
COMMITTEE FOR AERONAUTICS

Figure 3.-Stresses in simplified box.

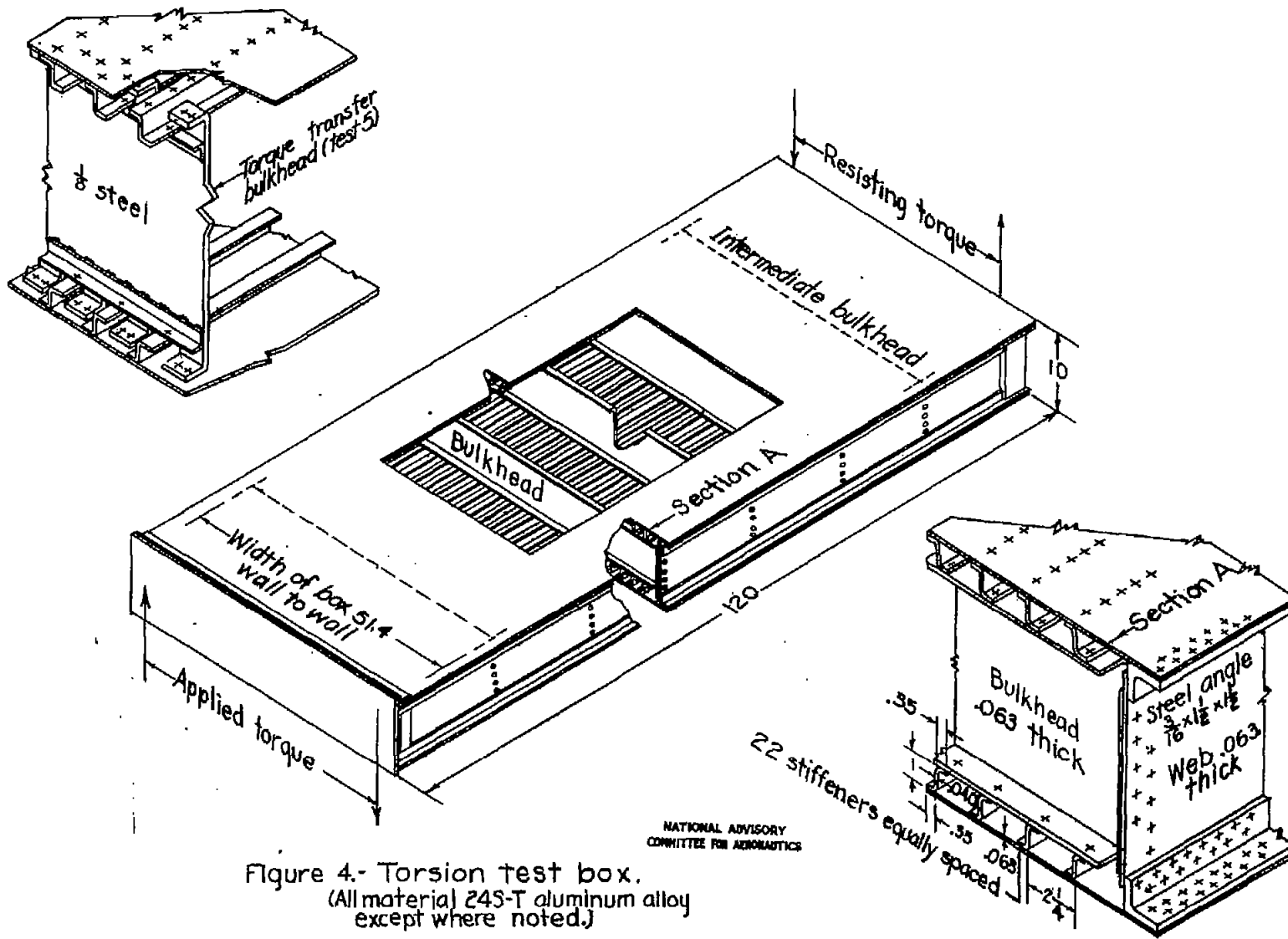


Figure 4.- Torsion test box.
(All material 24S-T aluminum alloy
except where noted.)

NATIONAL ADVISORY
COMMITTEE FOR AERONAUTICS

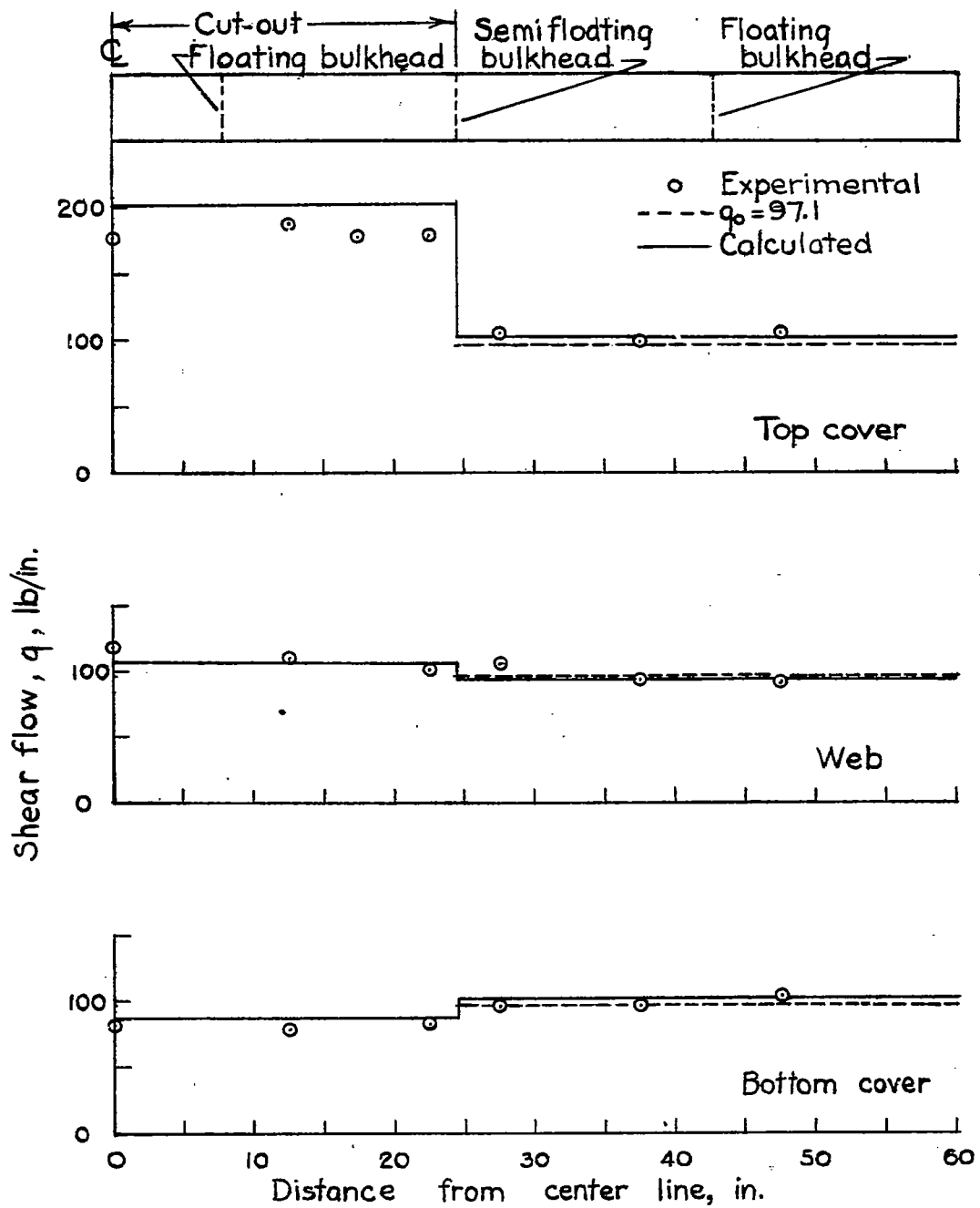


Figure 5.—Spanwise distribution of average shear flows.
Case I.

NATIONAL ADVISORY
COMMITTEE FOR AERONAUTICS

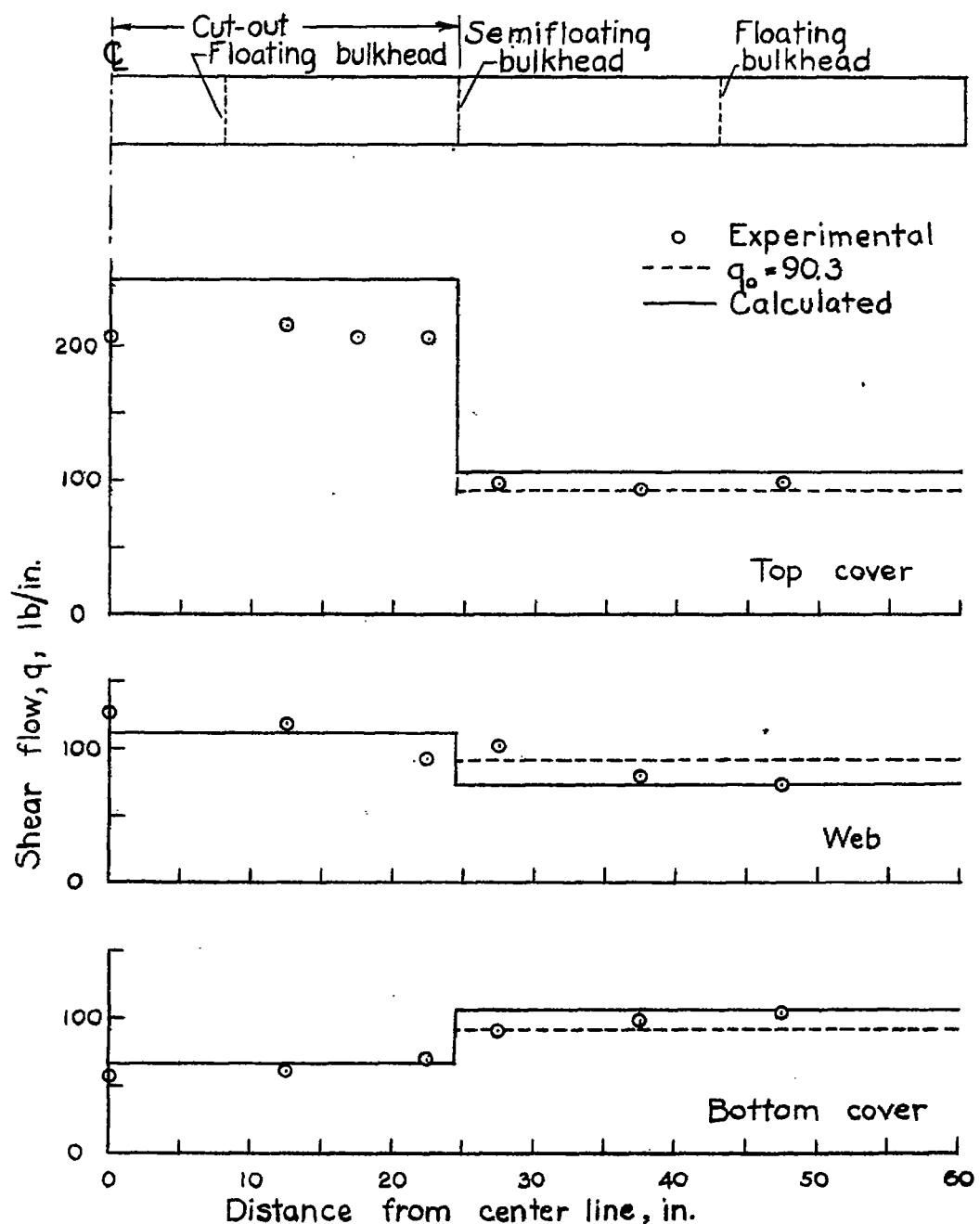


Figure 6.- Spanwise distribution of average shear flows.
Case 2.

NATIONAL ADVISORY
COMMITTEE FOR AERONAUTICS

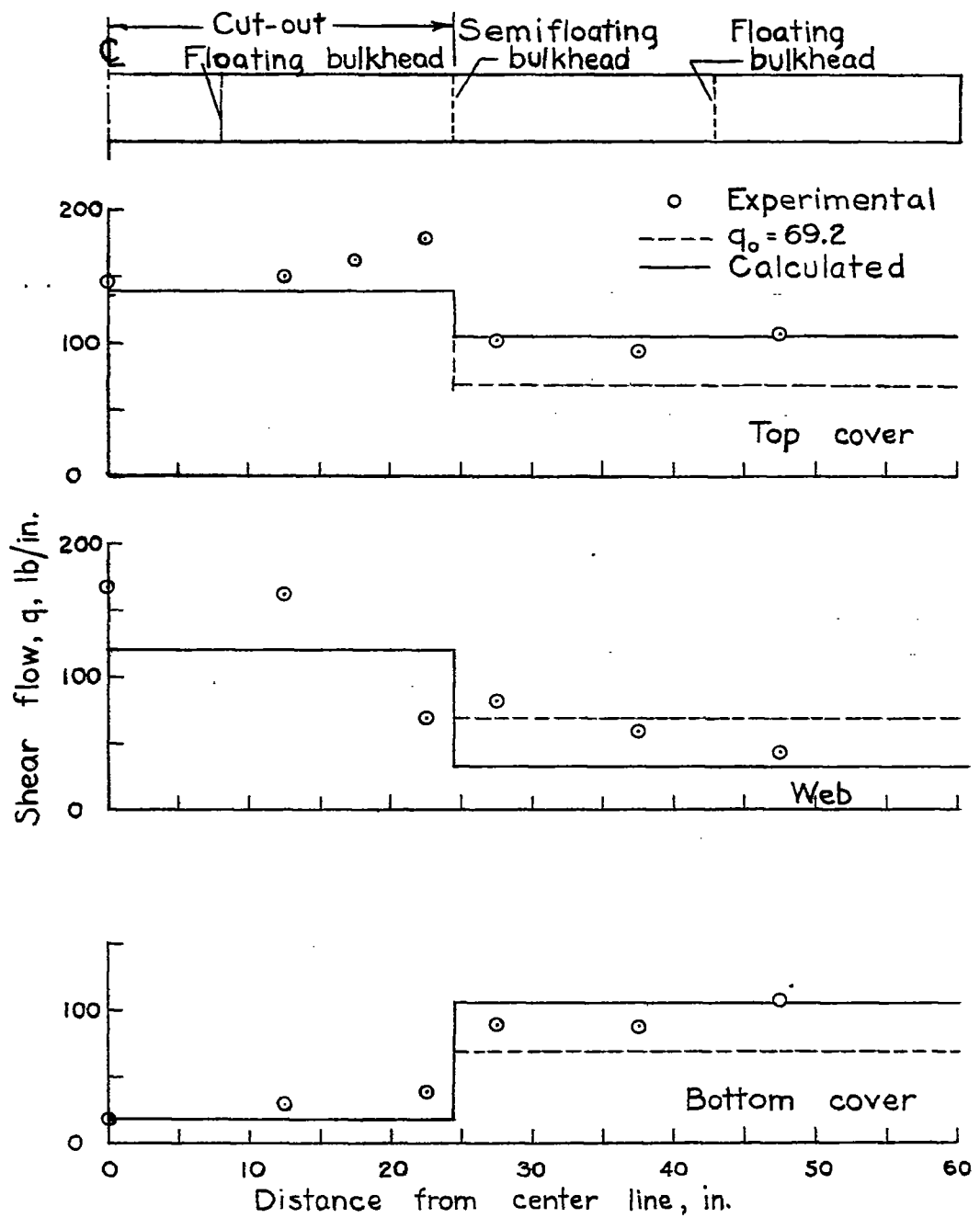


Figure 7.- Spanwise distribution of average shear flows.
Case 3.

NATIONAL ADVISORY
COMMITTEE FOR AERONAUTICS

Fig. 8

NACA TN No. 1066

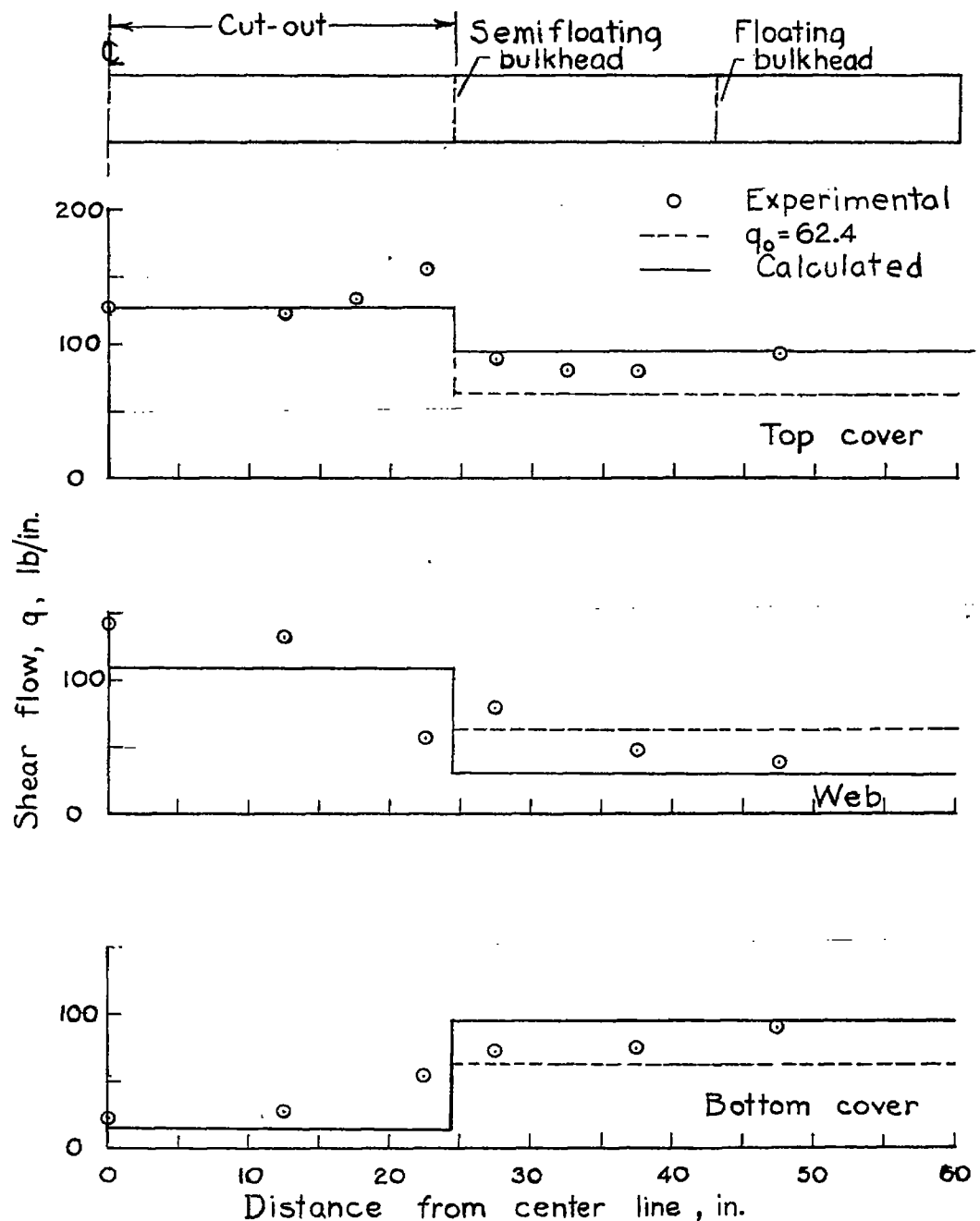


Figure 8.- Spanwise distribution of average shear flows.
Case 4.

NATIONAL ADVISORY
COMMITTEE FOR AERONAUTICS

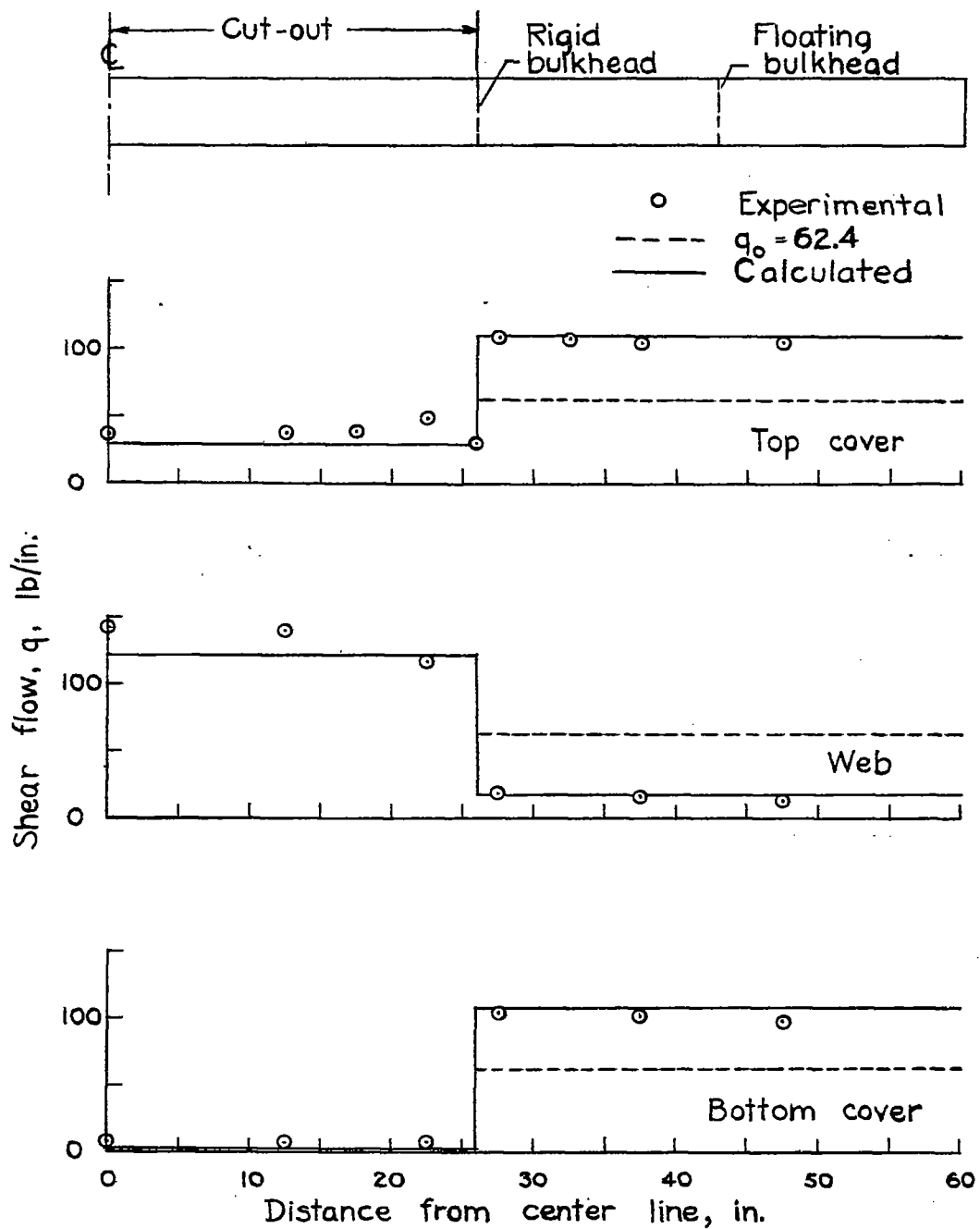


Figure 9.- Spanwise distribution of average shear flows.
Case 5.

NATIONAL ADVISORY
COMMITTEE FOR AERONAUTICS

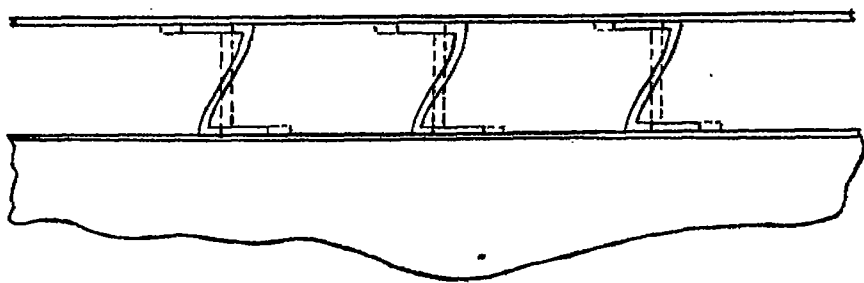
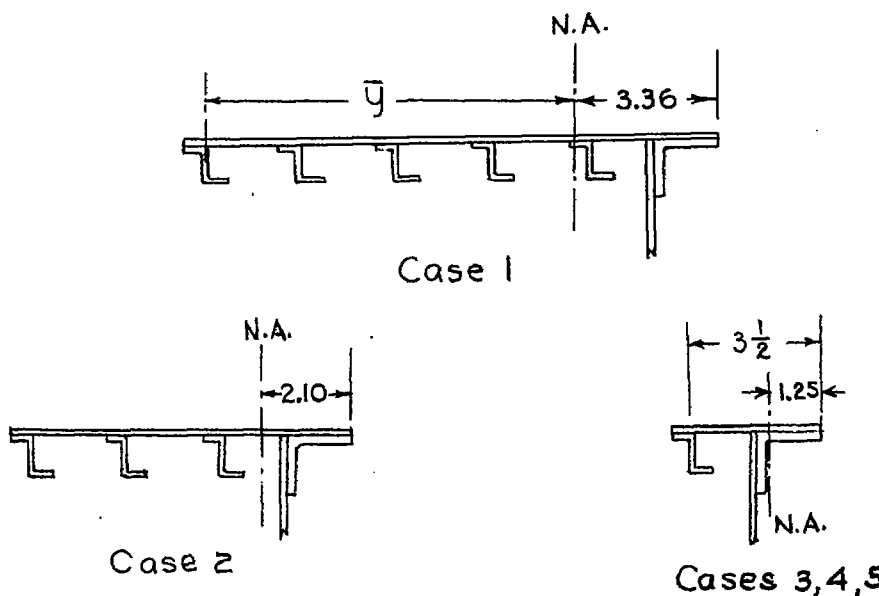


Figure 10.- Deformation of Z-stiffeners on floating bulkhead.



NATIONAL ADVISORY
COMMITTEE FOR AERONAUTICS

Figure 11.- Cross sections of cover at net section.

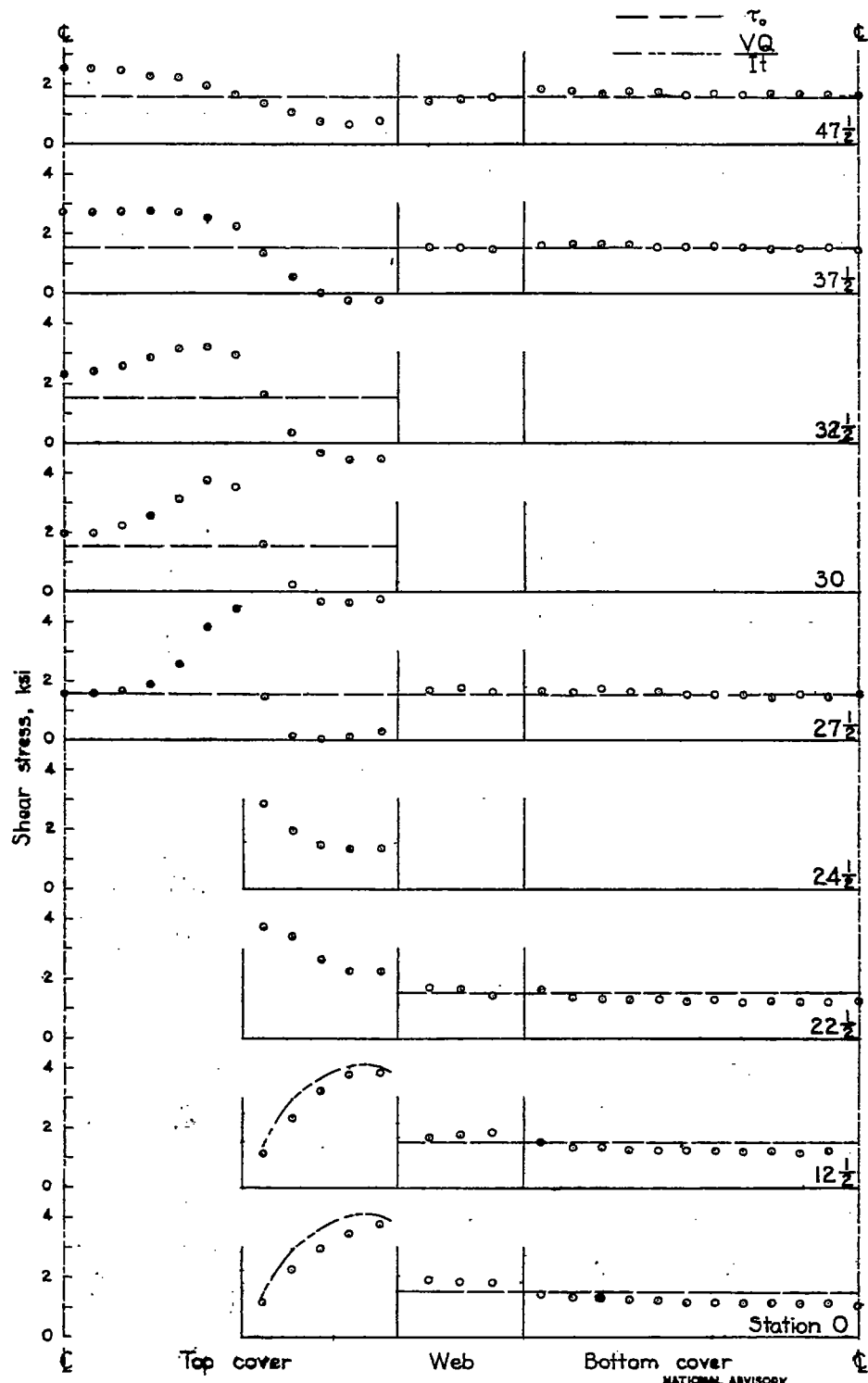


Figure 12.—Shear stress distribution over developed perimeter.
Case 1.

Fig. 13

NACA TN No. 1066

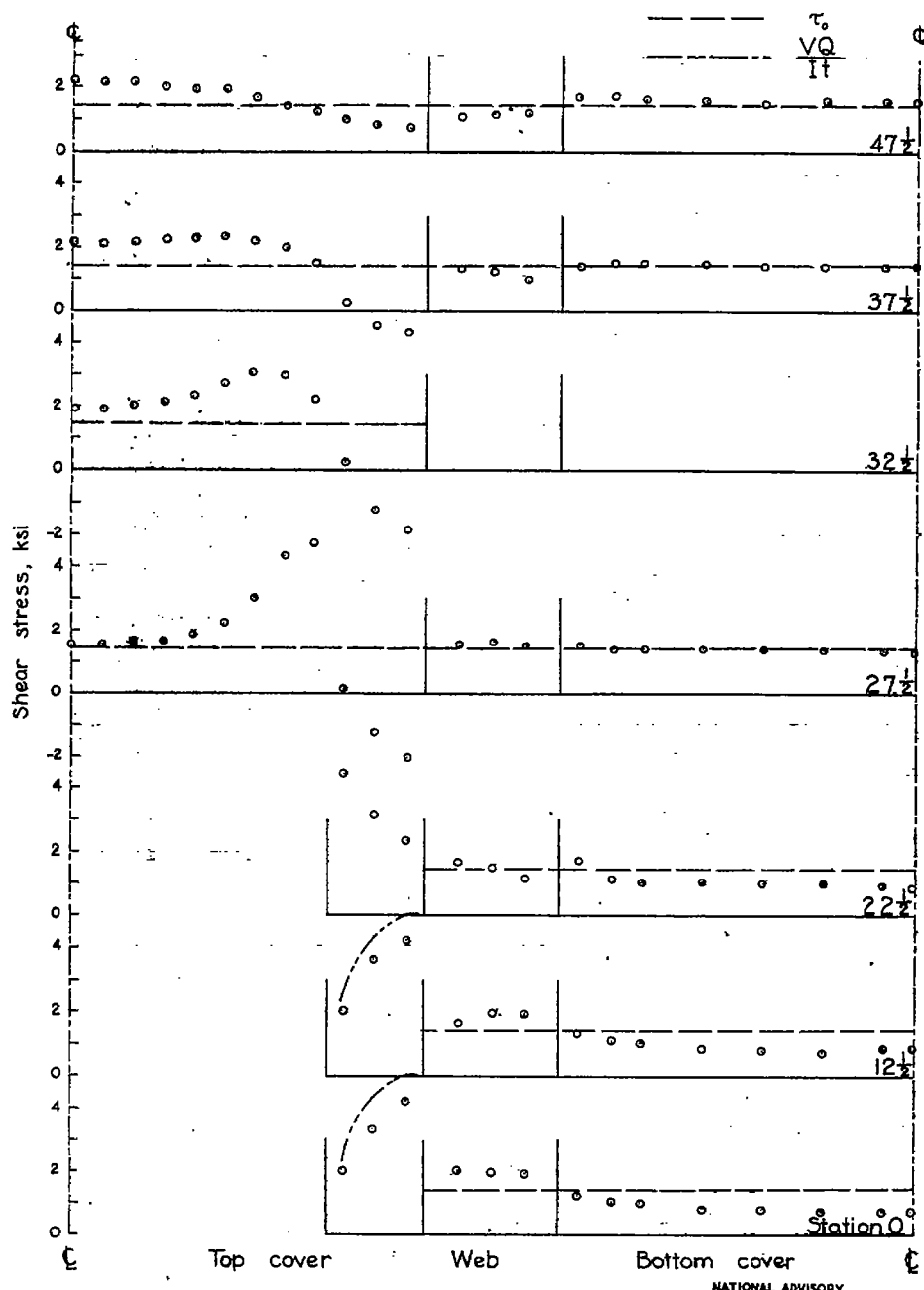


Figure 13.- Shear stress distribution over developed perimeter.
Case 2.

NATIONAL ADVISORY
COMMITTEE FOR AERONAUTICS

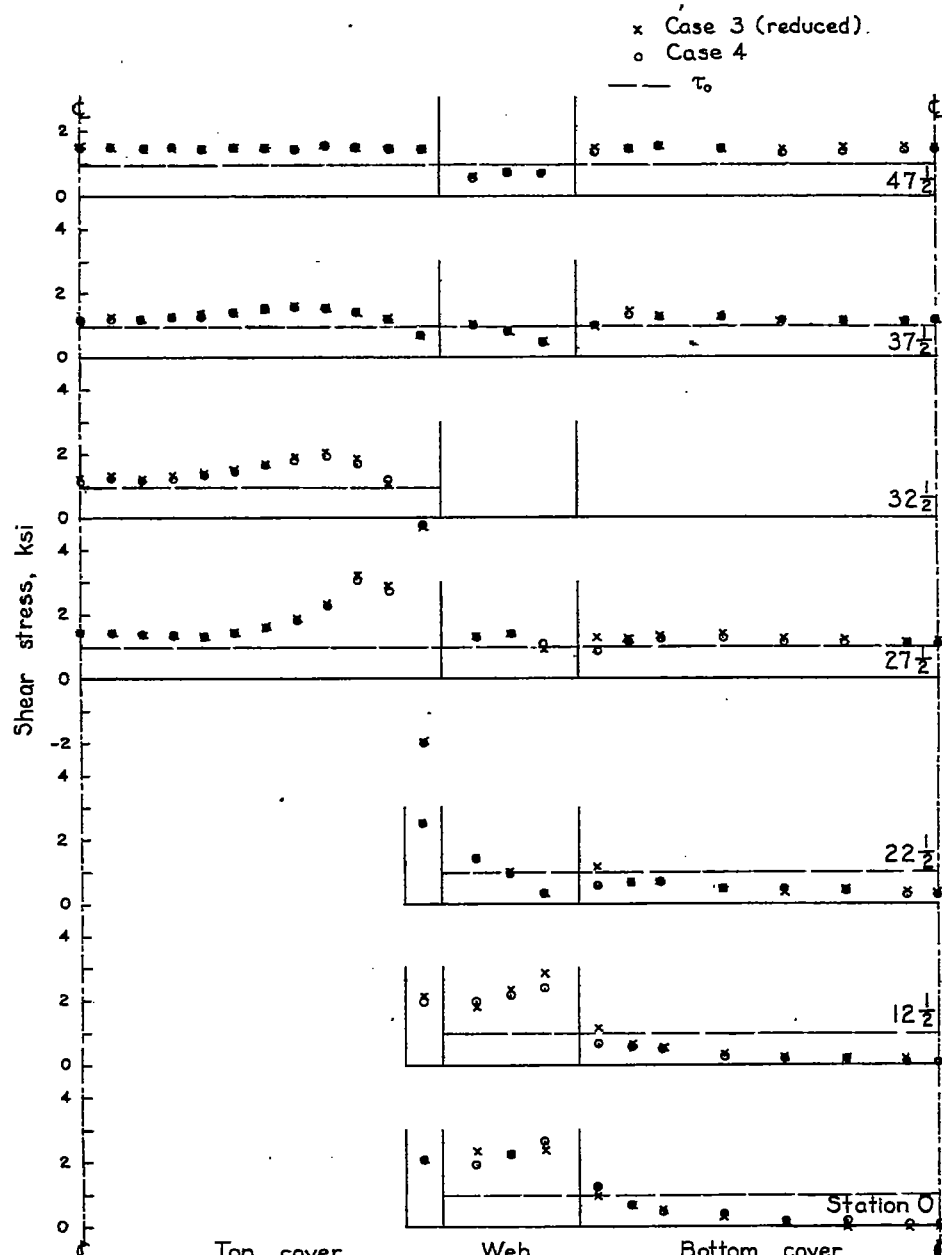


Figure 14.—Shear stress distribution over developed perimeter.
Cases 3 and 4.

NATIONAL ADVISORY
COMMITTEE FOR AERONAUTICS

Fig. 15

NACA TN No. 1066

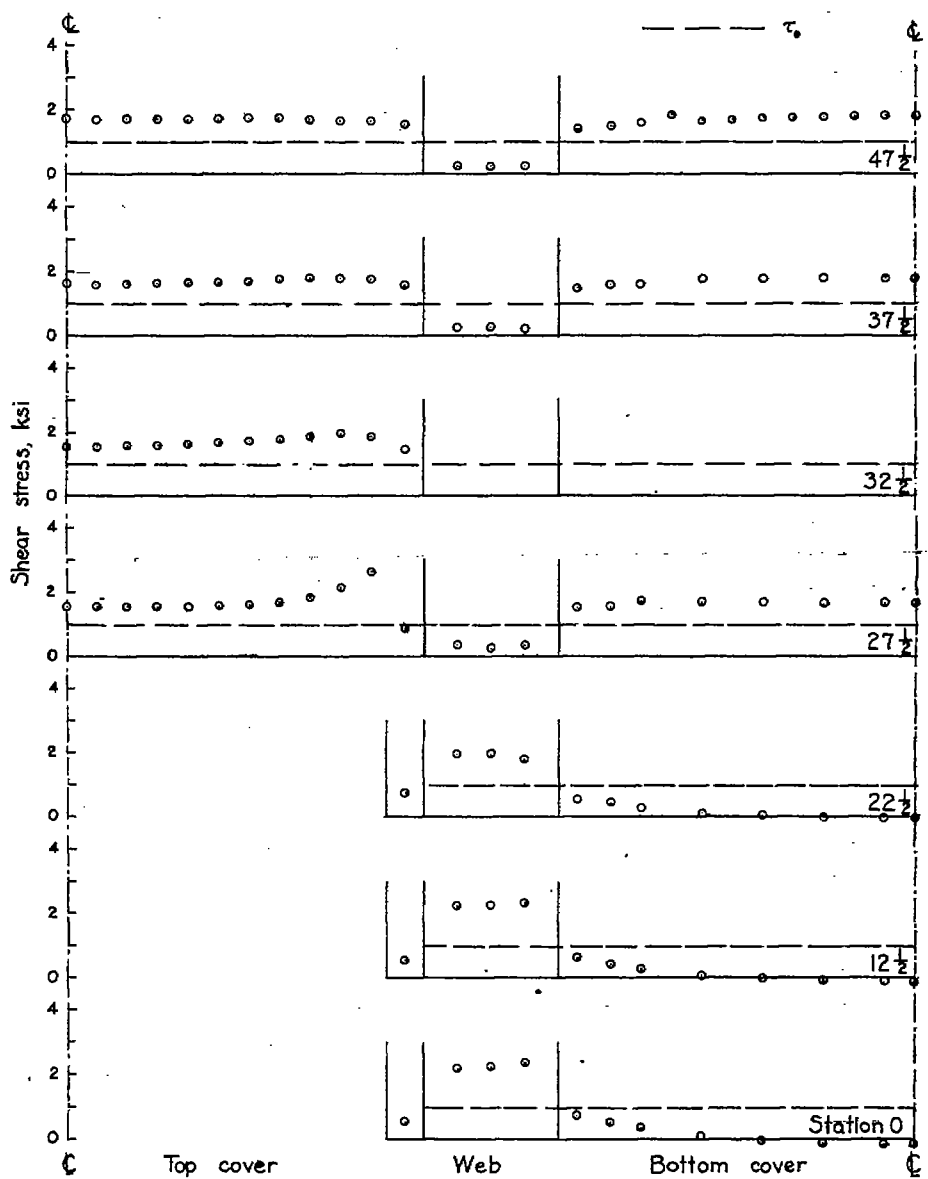


Figure 15.- Shear stress distribution over developed perimeter.

Case 5.

NATIONAL ADVISORY
COMMITTEE FOR AERONAUTICS

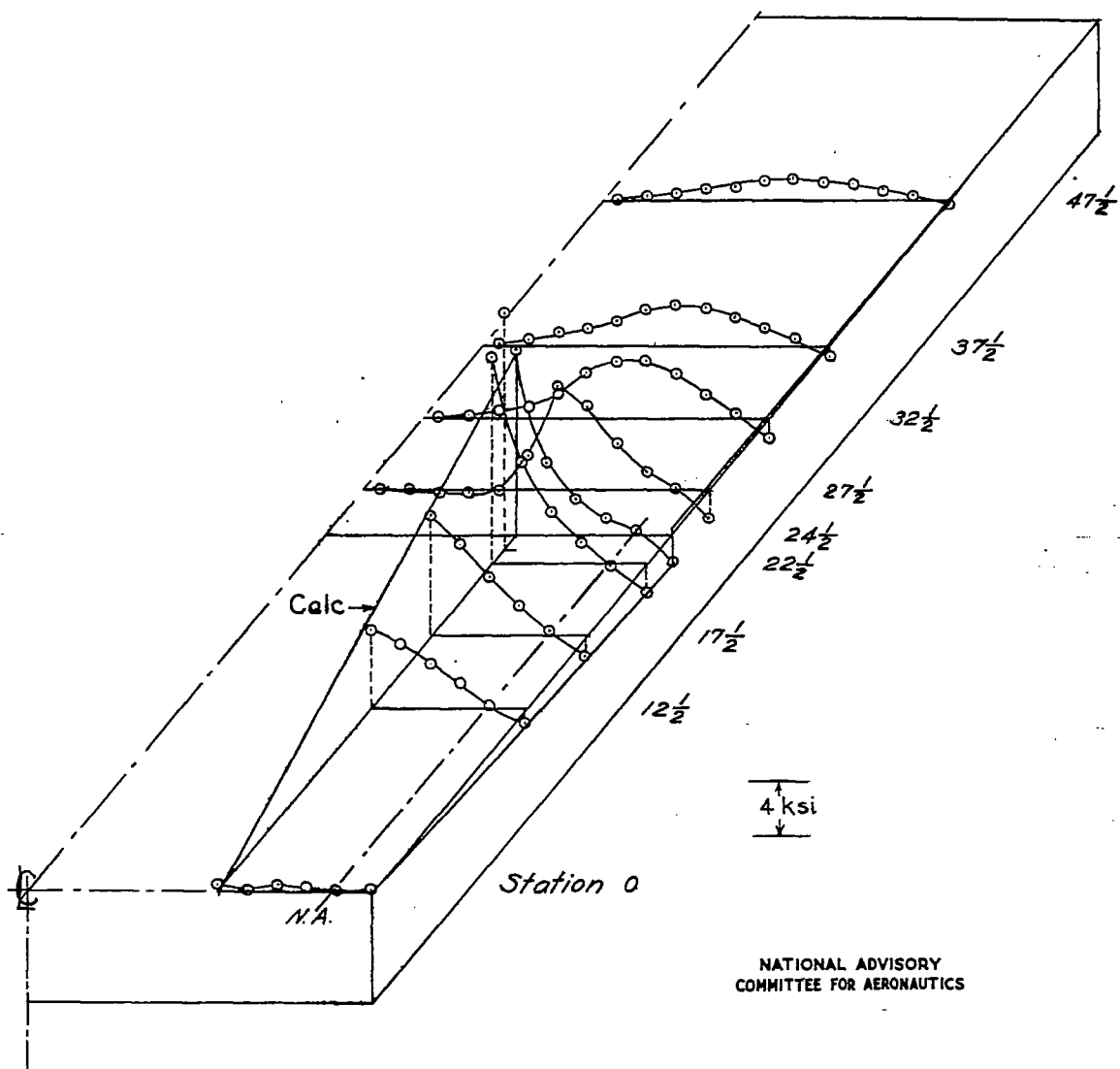
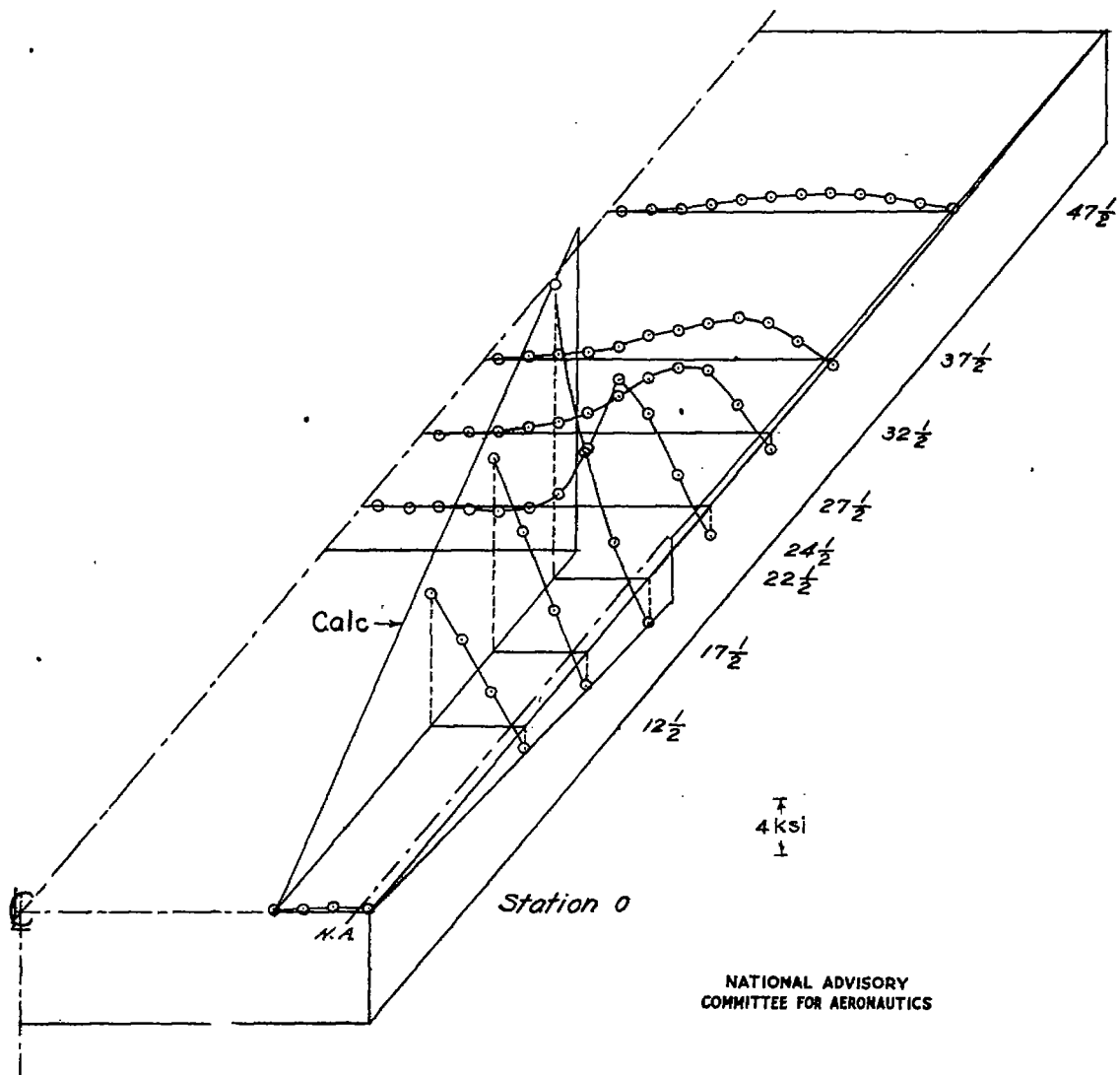


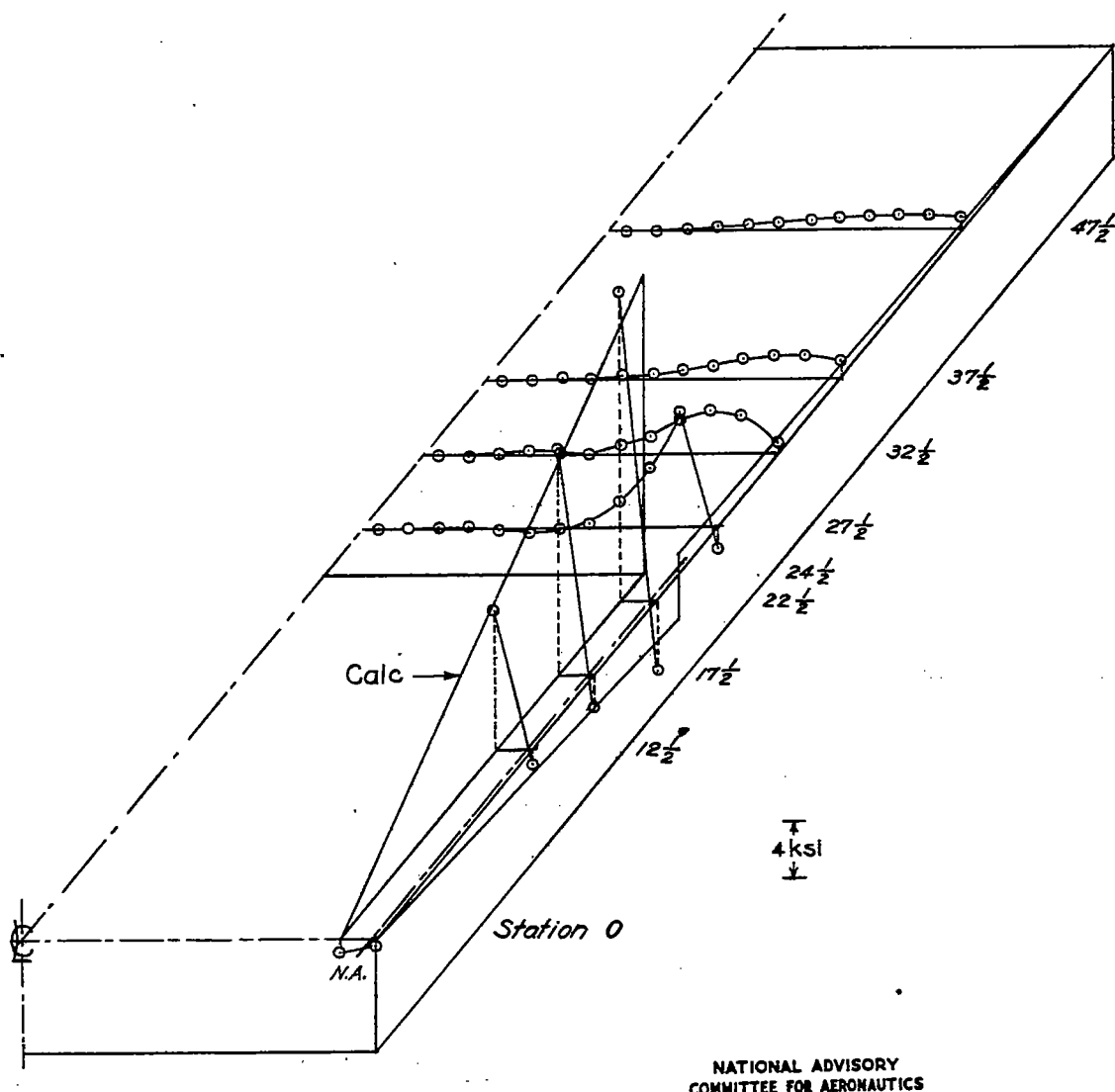
Figure 16.- Stringer stress distribution in top cover.
Case 1.



NATIONAL ADVISORY
COMMITTEE FOR AERONAUTICS

Figure 17.- Stringer stress distribution in top cover.

Case 2.



NATIONAL ADVISORY
COMMITTEE FOR AERONAUTICS

Figure 18.- Stringer stress distribution in top cover.
Case 3.

Fig. 19

NACA TN No. 1066

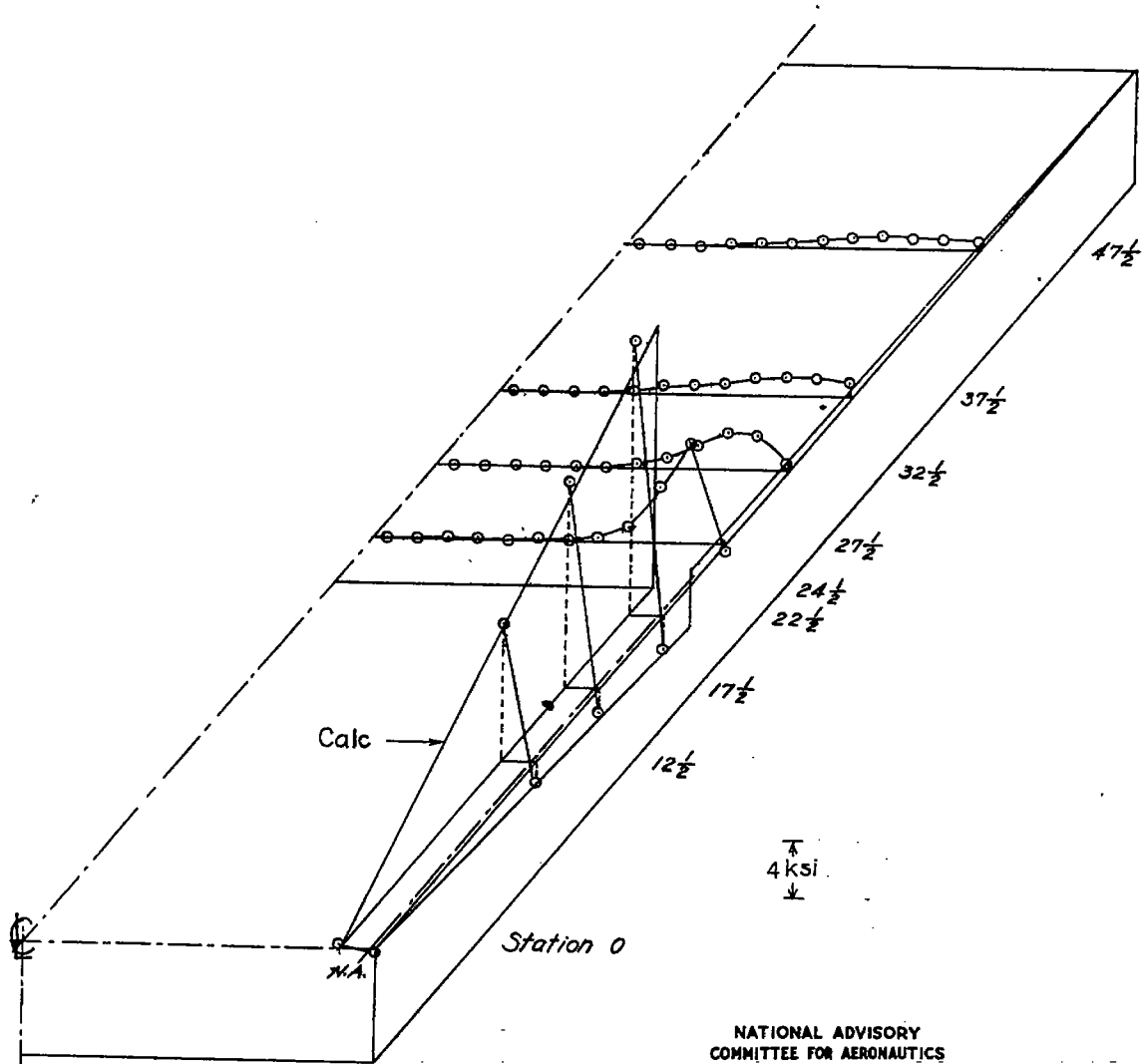


Figure 19.- Stringer stress distribution in top cover,
Case 4.

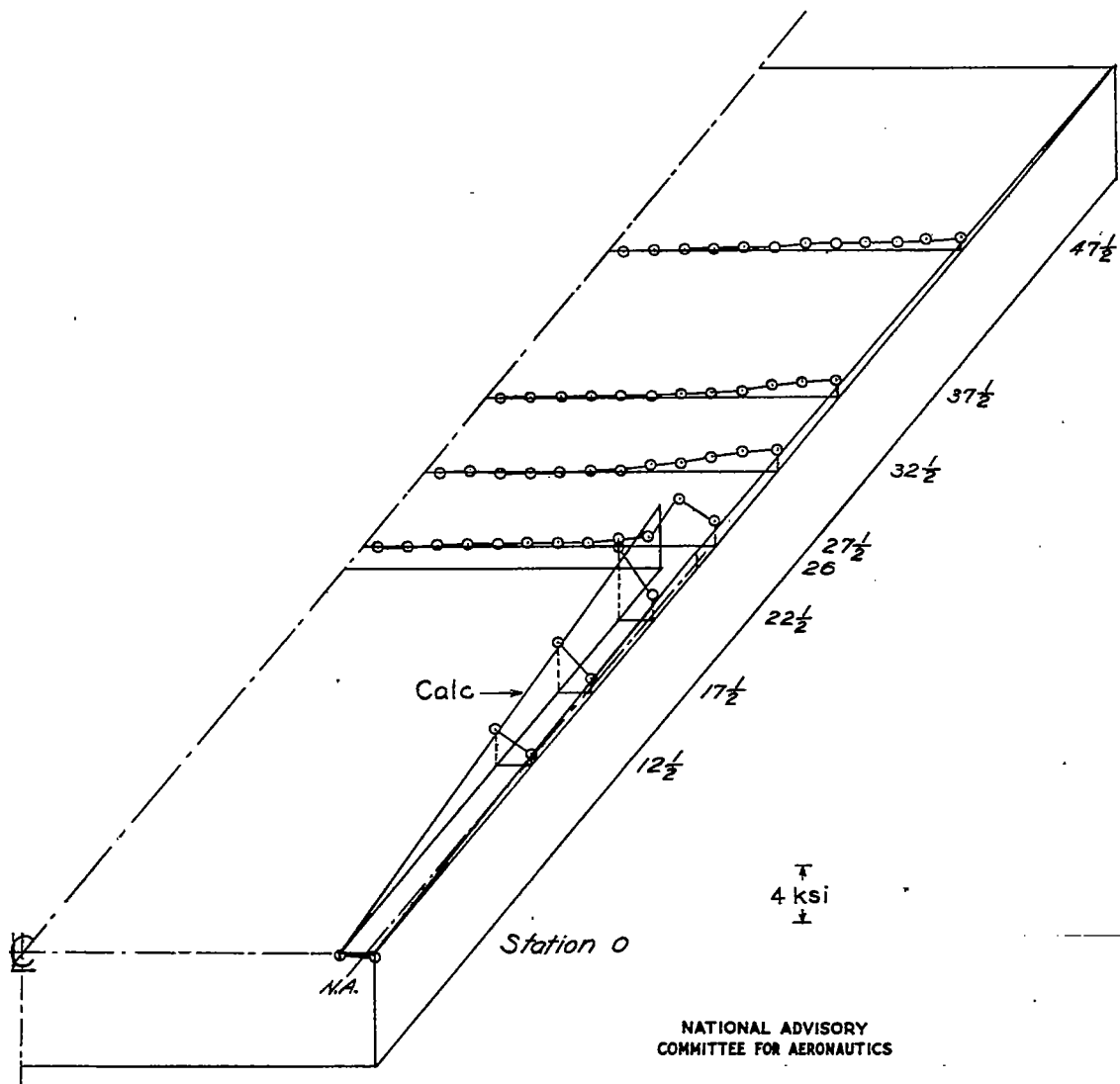


Figure 20.- Stringer stress distribution in top cover.
Case 5.

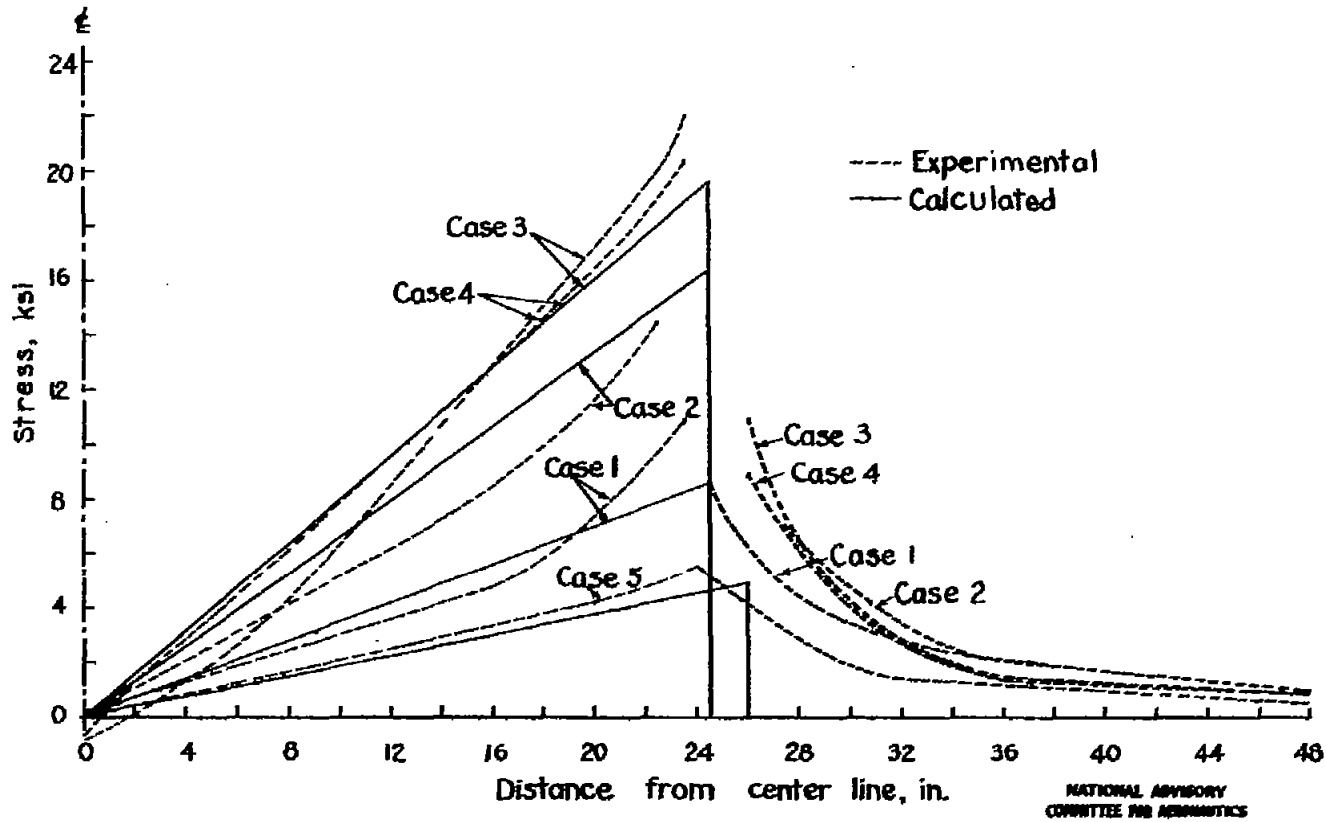


Figure 21.- Comparison of calculated and experimental stresses in coaming stringer.
All cases reduced to same torque.